ELSEVIER

Journal of Nuclear Materials 244 (1997) 251–257

journal of nuclear materials

Amorphization of U_3Si by ion or neutron irradiation

R.C. Birtcher [a,*], J.W. Richardson Jr [b], M.H. Mueller [b]

[a] *Materials Science Division, Argonne National Laboratory, Argonne, IL 60439, USA*
[b] *Intense Pulsed Neutron Source Division, Argonne National Laboratory, Argonne, IL 60439, USA*

Received 5 February 1996; accepted 19 June 1996

Abstract

Changes in crystal structure of U_3Si during irradiation have been monitored by diffraction techniques. Neutron diffraction was used to follow crystallographic changes produced by uranium fission during neutron irradiation at 30°C. The uranium fission fragments produce tracks of damage in the form of amorphous zones. Strain from the small volumes of amorphous material drives a transformation of the U_3Si crystal structure from the tetragonal to the cubic phase. Lattice strains develop at an initial rate of $(2.20 \times 10^{22}$ fissions/$m^3)^{-1}$ or $(0.076$ dpa$)^{-1}$, and the total lattice volume change after amorphization is $+2.0\%$ in U_3Si. At high doses, plastic flow in the amorphous volume fraction relieves strain in the remaining crystalline volume fraction of U_3Si. Complete amorphization of U_3Si occurs between 0.85 and 1.11×10^{23} fissions/m^3 or 0.29 to 0.38 dpa. Electron diffraction during in situ 1.5 MeV Kr ion irradiation was used to determine the doses required for amorphization of both U_3Si at temperatures above 30°C. As with fission fragments, individual Kr ions produce amorphous volumes that coexist with strained crystalline material. The temperature limit for complete amorphization is 290°C for U_3Si. The same amount of damage is required for amorphization of U_3Si or U_3Si_2 by ion or neutron irradiation.

1. Introduction

High density intermetallic compounds have been considered for use in high power-density nuclear applications or lower power-density reduced enrichment applications. Catastrophic swelling, that can occur at high fuel loadings, prevents their use in many such applications [1]. The catastrophic swelling is due to plastic flow of amorphous material during irradiation [2]. Amorphization of U_3Si was first reported following neutron irradiation [3]. This result was confirmed for neutron irradiation [4–11] and achieved during ion irradiation [12–16]. Changes in atomic volume of U_3Si produced by amorphization, determined by diffraction techniques, show great scatter and are all a small fraction of the value determined by bulk density measurements [7].

In this work we utilize high resolution neutron diffraction following neutron irradiation and in situ transmission electron microscopy with electron diffraction during Kr ion irradiation to follow systematically the crystallographic changes in U_3Si as it becomes amorphous during irradiation. The two types of irradiations demonstrate the universality of the amorphization. Ion irradiation provides a rapid and relative simple way to irradiate these materials, while neutron bombardment allows use of bulk specimens. The combination of these scattering and damaging techniques provides access to a deeper understanding of radiation-induced amorphization of these materials. These results resolve the controversies regarding variation in the X-ray volume changes and their disagreement with bulk volume changes. Comparisons are made to a similar study of ion and neutron irradiated U_3Si_2 [17].

2. Experimental

Experimental techniques employed in this work were the same as used during the study of the amorphization of U_3Si_2 [17]. Specimens for electron microscopy observa-

* Corresponding author.

PII S0022-3115(96)00741-6

tions during ion irradiation were produced from alloys of depleted uranium and silicon that were arc melted together. The U_3Si alloy was intentionally made Si rich in order to avoid precipitates of pure uranium. The ingots were heat treated at 1075 K for 72 h producing a martensite phase material containing dispersed small U_3Si_2 precipitates [6]. The ingots were sliced into 400 μm thick wafers and TEM disks 3 mm in diameter were core-drilled from the wafers and jet-polished to perforation [18]. The only defects observed before irradiation were isolated dislocations and grain boundaries.

In-situ ion irradiations, that allowed changes in one area to be monitored during an entire irradiation, were performed at the HVEM-Tandem Accelerator Facility [19] which consists of a modified Kratos/AEI EM7 high voltage electron microscope (HVEM) and a 2 MV tandem National Electrostatics ion accelerator. Irradiations were performed with 1.5 MeV Kr ions at dose rates between 3 and 8×10^{15} Kr/m^{2}s. TRIM95 damage calculations [20] using a 20 eV threshold energy for U_3Si yield 0.549 dpa/10^{18} Kr/m^2. A value of 20 eV was used for the displacement threshold since there is no experimental determination. Average damage rates in 100 nm thick U_3Si specimens were 3×10^{-3} dpa/s. The highest temperature increase recorded by a thermocouple on the specimen holder during ion irradiation was less than 20°C. The electron energy in the HVEM was maintained at 300 kV that is below the 700 keV electron energy required to produce visible damage in U_3Si [21].

Amorphization during ion irradiation was discernible by diffuse rings in the electron diffraction pattern. Because U_3Si is locally amorphized by individual ions, a diffuse ring was detectable in the diffraction pattern after any ion dose. Detection of the onset of amorphization was limited only by the visibility of a weak diffuse ring in the presence of intense diffraction spots. Such a diffuse ring was observed after doses as low as 3×10^{16} Kr/m^2 or 0.015 dpa. Similarly determination of the complete amorphization dose was limited by the ability to detect the disappearance of all Bragg diffraction spots from a diffraction pattern containing several intense diffuse rings. For this reason, the amorphization dose was determined by examination of electron diffraction micrographs and not from the viewing screen in the HVEM. The complete amorphization dose was determined from the first electron diffraction micrograph that did not contain discernible Bragg diffraction spots from crystalline material. These determinations are somewhat subjective, but the same procedure was used in all cases and the results are internally consistent. Because discrete observations were made, the complete amorphization doses are uncertain by an irradiation step or approximately 5%.

U_3Si specimens for neutron irradiation were fabricated from high purity Si and highly depleted uranium, 0.022 at% ^{235}U by arc melting and crushing the ingot into 50 to 150 μm in diameter powder. As with the TEM specimens, the U_3Si alloy was intentionally made Si rich in order to avoid precipitates of pure uranium. The U_3Si powder was annealed at 1075 K for 72 h, and then doubly encapsulated in thin wall vanadium cans that had been evacuated and filled with He gas. The Si rich U_3Si powder contained precipitates of U_3Si_2 (< 15 vol%) and the uranium oxides UO and UO_2 (< 5 vol%) introduced by annealing. The swelling behavior of these powders, roll-bonded between aluminum plates, during high dose neutron irradiation has been previously studied [1].

Neutron irradiations were performed at IPNS in a room temperature facility located adjacent to the neutron source [22]. Neutrons were produced as the result of 450 MeV protons striking a uranium target. The neutron spectrum for this facility is characteristic of a reactor neutron spectrum with the addition of neutrons having energies up to 450 MeV. Damage in the specimens was primarily produced by uranium fission in a manner identical to damage production in operating nuclear reactor fuel. The nuclear-reaction cross sections for fast and thermal fission were determined by standard activation techniques to give a fission rate of 5.39×10^{-27} fissions/uranium/proton for the uranium isotope ratio found in the specimens. The irradiations were performed in small steps, U burn-up $< 3 \times 10^{-8}$, in order to closely follow changes in the crystal structure, and total uranium burn-up was about 2×10^{-6}. On average, the fission fragments have masses of 95 and 135 amu with kinetic energies of 95 and 70 MeV. Calculations of defect production by ions equivalent to the average fission fragments were made using TRIM95 [20] with a 20 eV threshold energy; the same as used for the 1.5 MeV Kr ion irradiations. The damage calculations for the ion and neutron irradiations scale with the threshold energy used, and the absolute value of the threshold energy will not affect comparison of the two types of irradiations. For the neutron irradiations, the calculations yield 0.345 dpa/(10^{23} fissions/m^3), and the average damage rate was 4×10^{-8} dpa/s.

Time-of-flight diffraction pattern was measured on the general purpose powder diffractometer (GPPD) at IPNS after each neutron irradiation step and an appropriate time for radioactive decay (as long as 150 days). The scattering data were analyzed using the Rietveld profile refinement technique [23]. The GPPD simultaneous collects scattered neutrons from 144 detectors grouped at fixed scattering angles of $2\Theta = \pm 148°$, $\pm 90°$, $\pm 60°$, $+30°$ and $-20°$ covering lattice spacings from 0.028 nm to 2 nm. For these experiments, only data from the highest resolution banks at $2\Theta = \pm 148°$ ($d \sim 0.04$ to 0.29 nm, $\Delta d/d$(FWHM) $\sim$ 0.0025) were processed. As the volume fraction of crystalline material decreased with increasing irradiation, data collection times increased from 12 h for unirradiated specimens to 48 h for highly irradiated specimens. The diffraction peak widths for the unirradiated specimen were the result of instrument resolution. Details of data collection and analysis are given by Jorgensen et al. [24].

3. Results

3.1. Ion irradiation

Heavy-ion irradiation of U_3Si or U_3Si_2 results in direct amorphization and the coexistence of both the crystalline and amorphous phases [15]. The doses of 1.5 MeV Kr ions required to fully amorphize U_3Si were determined from electron diffraction as a function of temperature, and the results are shown in Fig. 1. The amorphization dose increases sharply with increasing temperature as is typical for ion beam amorphization of intermetallic alloys and semiconductors. The maximum temperature at which specimens were amorphized is approximately 280°C for U_3Si. The fit to the amorphization data in Fig. 1 is based on the ion beam amorphization model of Dennis and Hale [25]. The temperature dependence arises from thermal recovery that increases with increasing temperature, of the volume amorphized by each ion. Based of this model, the critical temperature is 290°C for U_3Si.

An upper temperature limit for amorphization of 250°C has been reported for Ar irradiated U_3Si [13]. The difference in temperature limits for Ar and Kr ions has been observed for amorphization of other intermetallics by ion irradiation [26] and is due to the effect of cascade energy density produced by the differences in ion mass and energy deposition. Ion-irradiated, amorphous U_3Si recovered to the tetragonal phase at 290°C [13]. The recovery temperature of 290°C is expected to be higher than the ultimate temperature limit for amorphization by very dense cascades, and is not consistent with the critical amorphization temperature limit for U_3Si.

The Kr ion dose required for amorphization at room temperature is 0.28 dpa for U_3Si as compared to 0.32 dpa for U_3Si_2. These values are in agreement with the ranges determined during neutron irradiation. The differences are within the uncertainty associated with extending the TRIM calculations to the very high energies of the fission fragments and the dose step between which amorphization occurred during neutron irradiation.

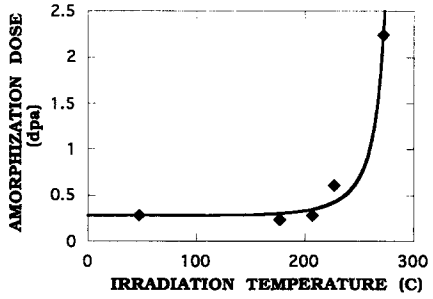

Fig. 1. Temperature dependence of the Kr ion dose for complete amorphization. The line is a fit based on the ion beam amorphization model of Dennis and Hale [25].

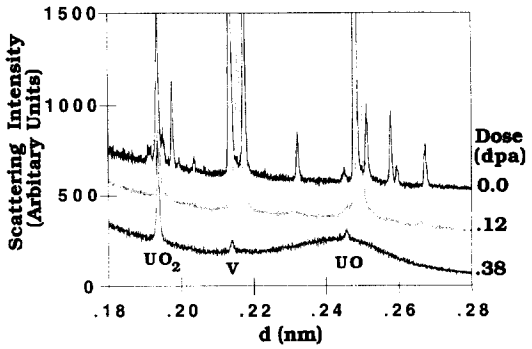

Fig. 2. Changes in the neutron scattering intensity from U_3Si produced by neutron irradiation. The curves have been normalized to the same total number of counts over the range shown. The irradiation doses in displacements per atom are indicated on the right side of the figure. The curves from before irradiation and after 0.12 dpa have been shifted by 1000 and 500 counts. Peaks from UO, UO_2 and V have been indicated.

3.2. Neutron irradiation

Neutron diffraction measurements before irradiation agree with the published structure [27]. We find that unirradiated U_3Si is tetragonal, space group I4/mcm, with $a = 0.603578$, $c = 0.869244$ nm, $c/a = 1.440$ and 16 atoms per unit cell. The atomic locations are: 4 U_I at $\pm(0, 1/2, 1/4)$; 8 U_{II} at $\pm(x, x + 1/2, 0)$ with $x = 0.22544$ and 4 Si at (0, 0, 1/4). The base layer ($z = 0$) contains only uranium atoms, the next layer ($z = 1/4$) contains an equal number of uranium and silicon atoms, and the sequence repeats. Sites in the pure uranium layer at $z = 0$ have positions shifted by $x\sqrt{2}$ away from the face-centered site at (1/2, 0, 1/2) and are rotated slightly relative to the base layer with the shift or rotation in the opposite sense in the layer at $z = 1/2$. This structure can be viewed as pseudo-cubic, in that if the U_{II} are shifted such that $x = 1/4$ and simultaneously the axial ratio (c/a) is reduced 1.8% to $\sqrt{2}$, U_3Si would have the cubic Cu_3Au type structure ($a_c = a_T/\sqrt{2} = c_T/2$). This transformation occurs upon heating to 1038 K [28].

Neutron diffraction patterns from powder U_3Si before and after neutron irradiation are shown in Fig. 2. The diffraction peak shapes from the unirradiated material are the result of instrument resolution limitations. Repeated irradiation produced structural changes that resulted in shifting and broadening of the Bragg peaks. In addition the Bragg peaks decreased in their intensities as the background intensity from diffuse scattering increased. The diffuse scattering arises from lattice damage and amorphous material in the specimens. The diffraction peak shifts arise from lattice distortions due to strains from defects and the increasing amorphous volume fraction. The only peaks resoluble from U_3Si after 0.292 dpa are at

0.214 nm and 0.252 nm. After the next irradiation step these peaks have disappeared into the undulating background scattering from amorphous U_3Si. The neutron irradiation dose at which all diffraction peaks have disappeared is between 0.85 and 1.11×10^{23} fissions/m^3 or 0.29 to 0.38 dpa for U_3Si compared to a range of 0.88 to 1.12×10^{23} fissions/m^3 or 0.30 to 0.38 dpa for U_3Si_2 [17]. The result for U_3Si is consistent with the results of Bethune who found amorphization of U_3Si between dose steps of 0.6 and 2×10^{23} fissions/m^3 [6].

The fractional changes in the lattice parameters from U_3Si are shown in Fig. 3 as a function of the amount of damage produced by the fission fragments. The behavior of U_3Si is quite different from that of U_3Si_2. In U_3Si the a-axis expands while the c-axis contracts, and the net volume change is positive. In U_3Si_2 the a-axis contracts strongly while the c-axis contracts slightly, and the net volume change is negative [17]. This difference explains the surface appearance after ion irradiation of U_3Si that contained second phase precipitates of U_3Si_2 [12,14]. In those works, and ours, the U_3Si_2 precipitates were recessed below the surface after the U_3Si had expanded and the U_3Si_2 had contracted after becoming amorphous.

At 30°C, U_3Si is directly amorphized by irradiation. Direct amorphization results in the volume fraction of amorphous material, f_A, increasing as

$$f_A = (1 - e^{-\sigma_A \Phi}) \quad (1)$$

where Φ is the neutron dose and σ_A is the initial rate of amorphization defined as the reciprocal of the dose in dpa required to amorphize a unit volume. The volume fraction of remaining crystalline material is given by $1 - f_A$. Lattice dilation arises from the long range strains due to cascade size volumes of amorphous material. At low doses when the volume fraction of amorphous material is small and localized in separated fission tracks, the lattice strain is equal to the product of the volume fraction of amorphous material times the volume dilation produced upon amorphization. At high doses when the volume fraction of crystalline material is small, volumes of crystalline material are embedded in amorphous material, and the situation is much more complex and it is not clear that lattice strain accumulates at a rate described by Eq. (1).

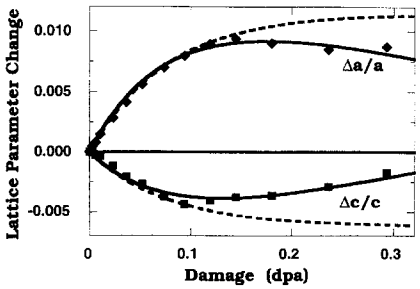

Fig. 3. Lattice parameter changes, $\Delta a/a$ (diamonds) and $\Delta c/c$ (squares), in U_3Si during neutron irradiation at room temperature. The lines are fits using Eq. (1) (dashed lines) or Eq. (2) (solid lines). The fitting parameters are given in the text and Table 1.

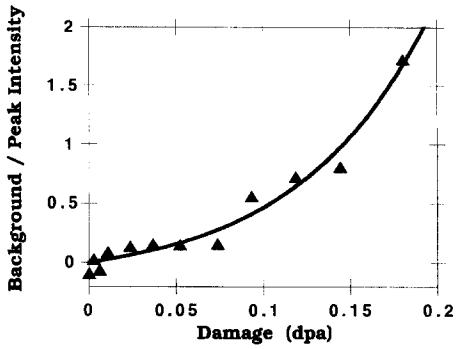

Fig. 4. Ratio of background intensity to peak intensity from U_3Si for scattering between d spacings of 0.212 nm and 0.220 nm. The line is a fit based on Eq. (1) as described in the text.

As the U_3Si specimen is amorphized, the scattering intensity in diffraction peaks decreases and the background scattering increases. Background scattering intensity for d spacings between 0.212 nm and 0.220 nm was determined by fitting a Lorenzian to the raw data. The ratio of integrated total background intensity to the integrated total intensities of the $\langle 220 \rangle$ and $\langle 004 \rangle$ reflections is shown in Fig. 4 as a function of the irradiation dose. The curve in Fig. 4 is a fit based on Eq. (1) with an initial rate of amorphization equal to $(0.076 \text{ dpa})^{-1}$ or $(2.20 \times 10^{22} \text{ fissions/m}^3)^{-1}$. The exponential increase of the background intensity indicates that amorphization is occurring directly within individual fission tracks and that the specimen is transforming from the crystalline state according to Eq. (1).

The two dashed curves in Fig. 3 are based on the assumption that the lattice parameter change is equal to the product of the unit strain produced by the volume change upon amorphization times the volume fraction of amorphous material given by Eq. (1). In this simple model and within the experimental uncertainty, the U_3Si lattice parameters change at the same rate, $(0.076 \text{ dpa})^{-1}$, as the background intensity increases in Fig. 4.

In our earlier work [17], the volume fraction of crystalline U_3Si_2 was determined from its scattering strength through Rietveld fits to the intensity of its Bragg peaks relative to those from the vanadium specimen container that remained crystalline throughout the entire irradiation [17]. The vanadium served as an internal standard for determining the number of neutrons scattered in each measurement. As more and more of the U_3Si_2 specimen was amorphized, the scattering intensity in diffraction peaks decreased and the background scattering increased as exponential functions of irradiation dose indicating that amorphization occurs directly within individual fission tracks. The volume fraction of crystalline U_3Si_2 was fit

with Eq. (1), and the initial rate of amorphization was also $(0.075\ \text{dpa})^{-1}$; the same as found for U_3Si.

The simple exponential fits to the lattice parameter changes in Fig. 4 indicate that for U_3Si the fractional increase in the a-axis saturates at 0.0115 while the c-axis contracts by 0.0062. The saturation value for the lattice volume expansion would be 0.0168 although the maximum achieved is 0.0157. Walker and Morel [13] found with X-ray diffraction after ion irradiation a saturation value for the lattice volume expansion of 0.012 based on a 0.4% shift of the $\langle 202 \rangle$ reflection. Consistent with this result, we find a total shift in the $\langle 202 \rangle$ d-spacing of 0.3725%, and from the complete diffraction pattern determine the change in the unit cell volume to achieve a maximum change of 0.0157 before declining as the specimen becomes progressively more amorphous. Bethune [6] found, using X-ray diffraction after a neutron dose equivalent to 0.17 dpa, that the a-axis had expanded by 0.0065 and the c-axis contracted by 0.0074 resulting in a volume expansion of 0.0056. After the same dose, we find the a-axis expansion to be 0.0087 and the c-axis contraction to be 0.0033 resulting in a volume expansion of 0.014. These X-ray diffraction results are based on an extremely limited number of reflections, and peak broadening plays a major role in their interpretation. In addition, the X-ray diffraction results are also sensitive to the surface treatment of the specimens, and cold work or surface deformation will result in the tetragonal to cubic transformation without amorphization [3,13]. The wide variations in the amorphization volume change determinations by experiments as well as the difference from a bulk volume change expansion of a 0.023 have been a long standing controversy. In general our results are in agreement with the X-ray diffraction results, and differences in the measured volume expansions are the result of stress relaxation in the remaining crystalline component due to plastic flow of the amorphous volume fraction. The apparent difference with the bulk volume expansion will be addressed in the next sections.

At damage levels greater that 0.1 dpa, the values of the lattice parameters of U_3Si deviate strongly from the simple exponential fits. The effect occurs for U_3Si_2 but is less noticeable [17]. These deviations indicate that lattice strains are being relaxed as the amorphous volume fraction increases and the remaining crystalline regions in the amorphous matrix become isolated from each other. Plastic flow of amorphous materials during irradiation is a universal behavior [29] that occurs in response to strain such as that associated with the volume change upon amorphization. During ion irradiation of thin TEM specimens, amorphous U_3Si undergoes rapid plastic flow while the flow rate in U_3Si_2 is much lower [2]. The neutron diffraction specimen used in this experiment consists of 50 to 150 μm diameter particles. For plastic flow to occur in our specimen, an amorphous volume must be connected to the surface so that it is free to expand. Thus strain in the crystalline fraction of the specimen shows an initial increase due to the volume change of embedded amorphous regions followed by a decrease in strain as the volume fraction of amorphous material increases and plastic flow occurs. On the basis of the simple exponential fits to the data in Fig. 3, strain relief becomes apparent in U_3Si, as well as in U_3Si_2 [17], when the volume fraction of amorphous material is 70%. At this concentration it is easy to visualize the remaining crystalline volumes becoming disconnected and the amorphous material yielding.

The rate of plastic flow during irradiation depends on the mechanical constraints imposed on the system. In an unconstrained amorphous system, plastic flow is proportional to the irradiation dose [29]. In order to gain insight into the strain relief, such a linear relaxation term was added to Eq. (1) so that the change in the a-axis lattice parameter is described as

$$\frac{\Delta a}{a} = -\alpha\Phi + \left.\frac{\Delta a}{a}\right|_{\max} * \left(1 - e^{-\sigma_A \Phi}\right) \qquad (2)$$

where α is a parameter related to the plastic flow rate whose sign is opposite to that of the change in lattice parameter, and $\Delta a/a|_{\max}$ is the maximum lattice strain along the a-axis that would be measured without strain relief due to plastic flow. A similar equation describes the changes in the c-axis direction. Values of the parameters for both U_3Si and U_3Si_2 are given in Table 1. A value of $\alpha = 0.018/\text{dpa}$ was found for both the a-axis and the c-axis of U_3Si, and a value of $\alpha = 0.0008/\text{dpa}$ for U_3Si_2. Due to the unknown mechanical constraints of the particles in the specimen, it is not clear how to interpret these values, however both α and unconstrained plastic flow during ion irradiation are much larger for U_3Si than for U_3Si_2 [2].

The volume change on amorphization, equal to the maximum lattice expansions without relaxation, is given by $2 * \Delta a/a|_{\max} + \Delta c/c|_{\max}$, where the subscripts refer to the a-axis and the c-axis. From the fit values in Table 1, the volume changes on amorphization are 0.020 for U_3Si and -0.022 for U_3Si_2. Bulk density measurements on

Table 1
Parameters derived by fitting Eq. (2) to lattice parameter changes determined by neutron diffraction

	$\Delta a/a\|_{\max}$	$\Delta c/c\|_{\max}$	$\Delta V/V\|_{\max}$	$1/\sigma_a$ (fissions/m^3)	$1/\sigma_a$ (dpa)	Plastic flow parameter α (dpa)$^{-1}$
U_3Si	0.0137	−0.0076	0.0198	2.78×10^{22}	0.076	0.018
U_3Si_2	−0.0106	−0.00094	−0.0221	2.24×10^{22}	0.076	0.0008

bulk U_3Si indicate a volume increase of 2.3% [7]. The values from bulk measurement and neutron diffraction are the same within their uncertainties, and there is no indication of excess vacancies [30] or voids [13] upon amorphization. Discrepancy of previous X-ray measurements with bulk density measurements was due to strain relief in the crystalline material through plastic flow of the amorphous volume fraction. Once strain relief initiates, the lattice parameters of the remaining crystalline material do not directly reflect the volume change on amorphization. No comparable bulk density measurements are available for U_3Si_2.

In addition to changes in lattice parameters, U_3Si undergoes a phase transformation to its high temperature cubic phase as atoms at the U_{II} position approach the idealized Cu_3Au position (1/4, 3/4, 0). This transformation has been detected by X-ray diffraction for neutron irradiation [6] and ion irradiation [12,13]. The cubic transformation is visible in Fig. 2 and is fully illustrated in Fig. 5 by the convergence of the $(220)_T$ and $(004)_T$ reflections to the cubic $(200)_C$, diffraction peak with increasing damage. For proposes of display, the $(220)_T$ peaks have been normalized to unity and the curves have been shifted vertically with increasing dose. Not apparent in this representation is the significant increase in the diffuse background scattering with increasing dose that is shown in Fig. 4. The apparent increase in noise with increasing irradiation dose is due to the decreasing volume fraction of crystalline material contributing to the diffraction peaks relative to the increasing scattering from defects and amorphous volume fraction contributing to background scattering. The d spacings of the $(220)_T$ and $(004)_T$ reflections are shown in Fig. 6 as a function of the irradiation dose. Extrapolation of these peaks positions to total convergence yields the high temperature, cubic-phase lattice parameter. After peak convergence at a dose of *0.1* dpa when the crystalline volume fraction has been reduced to *10%*, the $(200)_C$, diffraction peak continues to shift indicating additional lattice expansion at the rate of *6.1%*/dpa. The peak shifts indicate that the driving force of the transformation is the accumulation of homogeneous lattice strains without the direct formation of the cubic phase within the small volumes damaged by the fission fragments. Such direct formation of cubic material would be indicated by the growth of a [002] diffraction peak at 0.2156 nm rather than the merging of the two tetragonal peaks. Previous results based on X-ray diffraction claimed that the cubic phase was an intermediate phase before amorphization. We show here that this is not the case, and that strain from the amorphous volumes drives the tetragonal to cubic phase transformation much as internal stress from cold work or surface deformation can transform U_3Si to the cubic phase.

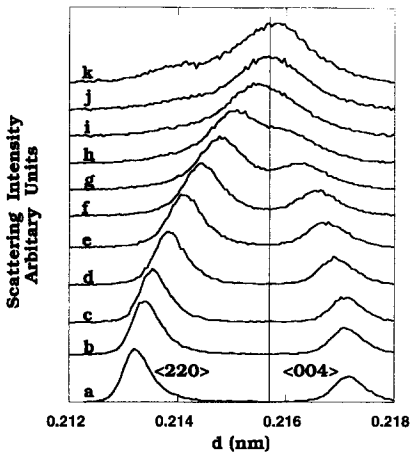

Fig. 5. Changes in the $(220)_T$ and $(004)_T$ reflections of U_3Si produced by neutron irradiation. Background intensities have been subtracted, and peak intensities have been normalized to unity. The different curves correspond to damage levels of: (a) 0; (b) 0.003; (c) 0.006; (d) 0.011; (e) 0.0235; (f) 0.037; (g) 0.052; (h) 0.074; (i) 0.093; (j) 0.119 and (k) 0.145 dpa. The vertical line at 0.2157 nm represents the $(200)_C$ reflection of the high temperature cubic phase.

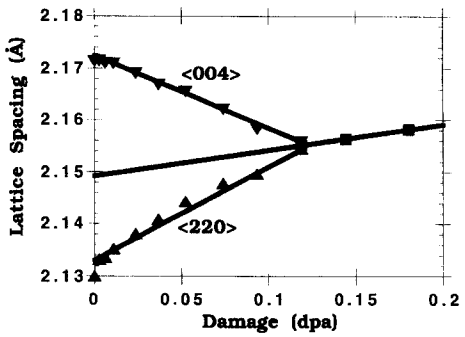

Fig. 6. Changes in the peak positions of the $(220)_T$ and $(004)_T$ reflections of U_3Si produced by neutron irradiation.

4. Conclusions

Diffraction techniques were used to follow crystallographic changes in U_3Si during neutron and ion irradiations. The temperature limit for amorphization by Kr ion irradiation is 290°C for U_3Si compared to 240°C for U_3Si_2. The same amount of damage, approximately 0.3 dpa, is required for ion beam amorphization of U_3Si or U_3Si_2 at room temperature.

During neutron irradiation at room temperature, amorphization by neutron irradiation of both U_3Si or U_3Si_2 is complete after a dose between 0.85 and 1.11×10^{23} fissions/m^3 or 0.29 to 0.38 dpa. The initial rate of amorphization by neutron irradiation, $(2.20 \times 10^{22}$ fissions/m$^3)^{-1}$ or $(0.076$ dpa$)^{-1}$, is the same for both alloys. Internal stress, induced by the expansion of the amorphous volume fraction, drives a transformation of

crystalline U_3Si from the tetragonal to the cubic phase. The cubic phase is not an intermediate phase produced before amorphization. The volume dilation upon amorphization is +2.0% in U_3Si compared to a value of −2.2% in U_3Si_2. The unit cell expansion of U_3Si without mechanical relaxation would be the same as found by bulk density measurements. However, plastic flow of the amorphous volume fraction relaxes the strain in the remaining crystalline volume fraction leading to a decrease in the distortion of the unit cell. The relaxation rate in U_3Si is estimated to be 20 times that in U_3Si_2. The volume contraction in U_3Si_2 does not provide a driving force for plastic flow.

Acknowledgements

Work supported by the US Department of Energy, Office of Basic Energy Sciences, under Contract W-31-109-Eng-38 at Argonne National Laboratory and Contract DE-AC05-84OR21400 at Oak Ridge National Laboratory.

References

[1] G.L. Hofman, J. Nucl. Mater. 140 (1986) 256.
[2] R.C. Birtcher, C.W. Allen, L.E. Rehn and G.L. Hofman, J. Nucl. Mater. 152 (1988) 73.
[3] M.L. Bleiberg and L.J. Jones, Trans. Met. Soc. AIME 212 (1958) 758.
[4] M.A. Feraday, G.H. Chalder and K.D. Cotnam, Nucl. Appl. 4 (1968) 148.
[5] C.R. Hann, R.D. Leggett, M.A. Feraday and G.H. Chalder, J. Nucl. Mater. 31 (1969) 114.
[6] B. Bethune, J. Nucl. Mater. 31 (1969) 197.
[7] J.R. MacEwan and B. Bethune, Irradiation Damage in U3Si, presented at the Radiation Damage in Reactor Materials, IAEA, Vienna, 1969, Vol. II, p. 447.
[8] I.J. Hastings and R.L. Stoute, J. Nucl. Mater. 37 (1970) 295.
[9] I.J. Hastings, J. Nucl. Mater. 41 (1971) 195.
[10] B. Bethune, J. Nucl. Mater. 40 (1971) 205.
[11] J. Pelissier, G. Silvestre and L. Lombard, J. Nucl. Mater. 43 (1972) 93.
[12] D.G. Walker, J. Nucl. Mater. 37 (1970) 48.
[13] D.G. Walker and P.A. Morel, J. Nucl. Mater. 39 (1971) 49.
[14] P.F. Caillibot and I.J. Hastings, J. Nucl. Mater. 59 (1976) 257.
[15] R.C. Birtcher, L.M. Wang, C.W. Allen and R.C. Ewing, Disordering and Amorphization of U3Si and U3Si2, presented at the XIIth International Congress for Electron Microscopy, 1990, p. 534.
[16] R.C. Birtcher and L.M. Wang, Nucl. Instrum. Methods Phys. Res. B 59–60 (1991) 966.
[17] R.C. Birtcher, J.W. Richardson, Jr. and M.H. Mueller, J. Nucl. Mater. 290 (1996) 158.
[18] B.J. Kestel, Ultramicroscopy 25 (1988) 91.
[19] A. Taylor, J.R. Wallace, E.A. Ryan, A. Phillippides and J.R. Wroedel, Nucl. Instrum. Methods 189 (1981) 261.
[20] J.F. Ziegler, J.P. Biersack and U. Littmark, The Stopping and Range of Ions in Solids (Pergamon Press, New York, 1985).
[21] I.J. Hastings, J. Nucl. Mater. 56 (1975) 76.
[22] R.C. Birtcher, T.H. Blewitt, M.A. Kirk, T.L. Scott, B.S. Brown and L.R. Greenwood, J. Nucl. Mater. 108–109 (1982) 3.
[23] H.M. Rietveld, J. Appl. Cryst. 2 (1969) 65.
[24] J.D. Jorgensen, Jr., Faber J., J.M. Carpenter, R.K. Crawford, J.R. Hauman, R.L. Hitterman, R. Kleb, G.E. Ostrowski, F.J. Rotella and T.G. Worton, J. Appl. Cryst. 21 (1989) 321.
[25] J.R. Dennis and E.B. Hale, J. Appl. Phys. 49 (1978) 1119.
[26] J. Koike, P.R. Okamoto, L.E. Rehn and M. Meshii, J. Mater. Soc. 4(5) (1989) 1143.
[27] W.H. Zachariasen, Acta Cryst. 2 (1949) 94.
[28] P.L. Blum, G. Silvestre and H. Vangoyeau, C.R. 260 (1965) 5538.
[29] S. Klaumünzer, C. Li, S. Löffler, M. Rammensee, G. Schumacher and H.C. Neitzert, Radiat. Eff. Defects Solids (1989) 131.
[30] J.R. MacEwan and R.R. Meadowcroft, J. Nucl. Mater. 40 (1971) 311.